

Direct measurement of field-free molecular alignment by spatial (de)focusing effects

Yahui Feng,¹ Haifeng Pan,¹ Jia Liu,¹ Cheng Chen,¹ Jian Wu,^{1,2} and Heping Zeng^{1,*}

¹State Key Laboratory of Precision Spectroscopy, East China Normal University, Shanghai 200062, China

²jwu@phy.ecnu.edu.cn

*hpzeng@phy.ecnu.edu.cn

Abstract: We directly measure the field-free molecular alignment of various room-temperature molecular gases based on alignment-induced spatial focusing and defocusing effects. By imaging the spatial profile of a time-delayed probe pulse with increased and decreased local intensity at the beam center, the parallel and perpendicular molecular alignments are clearly characterized. Meanwhile, the electronic Kerr effect, weak plasma contribution and field-free molecular alignment impact could be distinguished from the measured signals.

©2011 Optical Society of America

OCIS codes: (320.7100) Ultrafast measurements; (190.7110) Ultrafast nonlinear optics.

References and links

1. F. Rosca-Pruna, and M. J. J. Vrakking, "Experimental observation of revival structures in picosecond laser-induced alignment of I₂," *Phys. Rev. Lett.* **87**(15), 153902 (2001).
2. H. Stapelfeldt, and T. Seideman, "Colloquium: Aligning molecules with strong laser pulses," *Rev. Mod. Phys.* **75**(2), 543–557 (2003).
3. V. Renard, M. Renard, S. Guérin, Y. T. Pashayan, B. Lavorel, O. Faucher, and H. R. Jauslin, "Postpulse molecular alignment measured by a weak field polarization technique," *Phys. Rev. Lett.* **90**(15), 153601 (2003).
4. A. Couairon, and A. Mysyrowicz, "Femtosecond filamentation in transparent media," *Phys. Rep.* **441**(2-4), 47–189 (2007).
5. Y.-H. Chen, S. Varma, A. York, and H. M. Milchberg, "Single-shot, space- and time-resolved measurement of rotational wavepacket revivals in H₂, D₂, N₂, O₂, and N₂O," *Opt. Express* **15**(18), 11341–11357 (2007).
6. R. A. Bartels, T. C. Weinacht, N. Wagner, M. Baertschy, C. H. Greene, M. M. Murnane, and H. C. Kapteyn, "Phase modulation of ultrashort light pulses using molecular rotational wave packets," *Phys. Rev. Lett.* **88**(1), 013903 (2001).
7. T. Kanai, S. Minemoto, and H. Sakai, "Quantum interference during high-order harmonic generation from aligned molecules," *Nature* **435**(7041), 470–474 (2005).
8. C. Vozzi, F. Calegari, E. Benedetti, J.-P. Caumes, G. Sansone, S. Stagira, M. Nisoli, R. Torres, E. Heesel, N. Kajumba, J. P. Marangos, C. Altucci, and R. Velotta, "Controlling two-center interference in molecular high harmonic generation," *Phys. Rev. Lett.* **95**(15), 153902 (2005).
9. J. Wu, H. Cai, H. Zeng, and A. Couairon, "Femtosecond filamentation and pulse compression in the wake of molecular alignment," *Opt. Lett.* **33**(22), 2593–2595 (2008).
10. Y.-H. Chen, S. Varma, and H. M. Milchberg, "Space- and time-resolved measurement of rotational wave packet revivals of linear gas molecules using single-shot supercontinuum spectral interferometry," *J. Opt. Soc. Am. B* **25**(7), 122–132 (2008).
11. H. Cai, J. Wu, A. Couairon, and H. Zeng, "Spectral modulation of femtosecond laser pulse induced by molecular alignment revivals," *Opt. Lett.* **34**(6), 827–829 (2009).
12. H. Cai, J. Wu, Y. Peng, and H. Zeng, "Comparison study of supercontinuum generation by molecular alignment of N₂ and O₂," *Opt. Express* **17**(7), 5822–5828 (2009).
13. J. Wu, H. Cai, Y. Tong, and H. Zeng, "Measurement of field-free molecular alignment by cross-defocusing assisted polarization spectroscopy," *Opt. Express* **17**(18), 16300–16305 (2009).
14. V. Renard, O. Faucher, and B. Lavorel, "Measurement of laser-induced alignment of molecules by cross defocusing," *Opt. Lett.* **30**(1), 70–72 (2005).
15. V. Lorient, E. Hertz, A. Rouzée, B. Sinardet, B. Lavorel, and O. Faucher, "Strong-field molecular ionization: determination of ionization probabilities calibrated with field-free alignment," *Opt. Lett.* **31**(19), 2897–2899 (2006).
16. I. V. Litvinyuk, K. F. Lee, P. W. Dooley, D. M. Rayner, D. M. Villeneuve, and P. B. Corkum, "Alignment-dependent strong field ionization of molecules," *Phys. Rev. Lett.* **90**(23), 233003 (2003).
17. N. Xu, C. Wu, Y. Gao, H. Jiang, H. Yang, and Q. Gong, "Measurement of the field-free alignment of diatomic molecules," *J. Phys. Chem. A* **112**(4), 612–617 (2008).
18. M. Centurion, Y. Pu, Z. Liu, D. Psaltis, and T. W. Hänsch, "Holographic recording of laser-induced plasma," *Opt. Lett.* **29**(7), 772–774 (2004).

19. J. Wu, H. Cai, H. Milchberg, and H. Zeng, "Molecular quantum wakes in the hydrodynamic plasma waveguide in air," *Phys. Rev. A* **82**(4), 043431 (2010).
 20. J. Wu, H. Cai, Y. Peng, Y. Tong, A. Couairon, and H. Zeng, "Control of femtosecond filamentation by field-free revivals of molecular alignment," *Laser Phys.* **19**(8), 1759–1768 (2009).
 21. G. P. Agrawal, *Nonlinear Fiber Optics* (Academic Press, San Diego, 2001).
 22. NIST chemistry webbook, <http://webbook.nist.gov/chemistry>.
-

1. Introduction

Periodic revivals of field-free molecular alignment [1–5] after impulsive rotational Raman excitation by an ultrashort laser pulse have attracted growing interest for its interesting applications in chemistry and ultrafast optics [6–12]. Many probing techniques have been applied to measure the molecular alignment, quantified by the statistic metric $\langle\langle\cos^2\theta\rangle\rangle$, which is greater, less than, and equal to 1/3 for parallel, perpendicular and random molecular alignment, respectively. Here θ is the angle between the molecular axis and the polarization of the aligning pulse. The weak field polarization technique [3,13] and cross-defocusing measurement [14,15] were successfully used to measure the alignment signals, obtaining a signal proportional to $(\langle\langle\cos^2\theta\rangle\rangle-1/3)^2$ rather than $\langle\langle\cos^2\theta\rangle\rangle$, where the parallel and perpendicular alignment revivals were hard to be directly distinguished since both of them showed increased signals from the measurement with respect to the random molecular orientation. Other methods such as supercontinuum spectral interferometry [5,10], Coulomb explosion of pre-aligned molecules [15,16], and a revised weak field polarization technique [17] could be used to get alignment signals proportional to $\langle\langle\cos^2\theta\rangle\rangle$ or $(\langle\langle\cos^2\theta\rangle\rangle-1/3)$.

In this paper, we present a simple and intuitive method based on alignment-induced spatial (de)focusing effects to directly characterize the field-free molecular alignment. Impulsive rotational Raman excitation induced molecular alignment experiences periodic revivals after the extinction of the pump pulse. The pre-aligned molecules show orientation-dependent refractive index changes, which can be considered as a newly established gas-phase nonlinear lens by considering the Gaussian-shaped spatial distribution of the pump pulse. Accordingly, a weak probe pulse propagating through the pre-aligned molecules undergoes spatial refractive index gradient, which modifies its spatial intensity property. This spatial modulation effect, extracted by detecting the local intensity of the central part of a weak probe pulse, is relevant to the molecular alignment degree and can be used to directly reconstruct the molecular alignment revivals. The measured results of field-free alignment of room-temperature N_2 , O_2 , air, NO, CO and CO_2 at atmosphere pressure are presented. Moreover, the electronic Kerr effect, the weak plasma and field-free molecular alignment impact on the modulation of the probe pulse differ in both time and intensity scales, which can be clearly distinguished.

2. Experimental setup

A schematic configuration of our experimental setup is shown in Fig. 1. The pulse from an amplified Ti:Sapphire laser system (~50 fs, 800 nm, 1 kHz) was split into two parts: one served as the excitation pulse for molecular alignment (M-pulse), the other passed through a β -barium borate (BBO) crystal (type-I, 29.2°-cut, 200- μ m-thick) to generate second harmonic (SH), acted as the weak probe pulse. The time delay between the M-pulse and probe pulse was precisely controlled by a motorized translation stage. A half-wave plate (HWP) located in the path of the M-pulse was used to rotate the polarization of the M-pulse with respect to that of the probe pulse. The M-pulse and probe pulse were focused by lenses of $f = 50$ and 40 cm, respectively, with their focal spots spatially overlapped collinearly at the center of a 20-cm-long gas cell, which was filled with different room-temperature gases at atmosphere pressure. After the gas cell, a couple of dichromatic mirrors were used to remove the M-pulse at 800 nm by reflecting the 400 nm probe pulse. The output beam profile of the probe pulse was imaged by an imaging system in 4- f configuration and then photographed by a charge coupled device (CCD) [18,19]. A variable attenuator was put in front of the CCD, making sure that the CCD worked well below its saturation level. The recorded spatial profile of the probe pulse was sent to a computer, where the local intensity at the beam center was integrated versus the

time delay which directly reflected the field-free molecular alignment revivals. As compared with the previous experiments based on the cross-defocusing effect [14,15], here the molecular alignment was collinearly probed and the spatial (de)focusing effect induced spatial variation of the probe pulse was directly imaged (rather than the molecule alignment diffracted far-field ones) and recorded by a CCD [13–15].

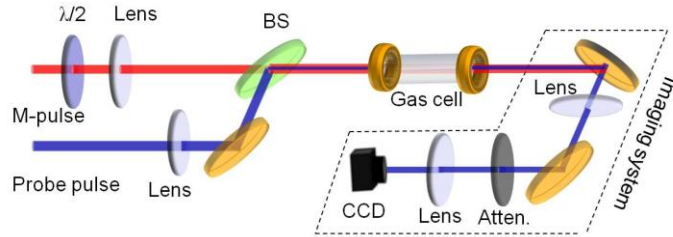


Fig. 1. Schematic configuration of the experimental setup. The M-pulse (red, 800 nm) and the probe pulse (blue, 400 nm) are combined at a beam splitter (BS) which is highly reflective at 400 nm and transmitted at 800 nm. The gas cell is filled with various room-temperature molecular gases at 1 atm. A 4-*f* imaging system is used to image the output spatial profile to a recording CCD.

3. Results and discussions

Since we measured the intensity variation of the weak probe pulse in a selected center part, there existed an inevitable background signal, which was in fact equivalent to the selected center part intensity of the probe pulse without any effects of molecular alignment (corresponding to the case of random molecular orientation). The alignment-induced intensity variation in the selected center part could thus be obtained by subtracting the background signal from the detected signal. Throughout the paper, a positive signal signifies the spatial focusing phenomenon, indicating that the molecules were aligned parallel to the polarization of the probe pulse for which a bright spot pattern in the center was observed, while on the other hand a ring probe beam pattern and a negative signal corresponds to spatial defocusing with perpendicular alignment. As a consequence, the perpendicular post-pulse transient molecular alignment revivals could be clearly different from the parallel ones.

Figure 2 shows the measured alignment signals of molecular O₂ (solid curves) under the excitation of M-pulse with the intensity of 4.6×10^{13} W/cm² when the M-pulse and probe pulses were polarized parallel and perpendicularly to each other, respectively. The signals consisted of a series of revivals after the vanishing of the M-pulse, giving rising to the spatial focusing or defocusing effects induced by the molecular alignment. Since the degree of alignment was sensitively proportional to the excitation pulse intensity before its saturation, the Gaussian-shaped transverse profile of the M-pulse produced a larger molecular alignment degree at the central part than that at its periphery. Then the parallel (perpendicular) molecular alignment revival with increased (decreased) refractive index introduced a spatial focusing (defocusing) effect which was equivalent to a positive (negative) lens and increased (decreased) the local intensity at the interaction part of the probe pulse. Such focusing and defocusing phenomena, depicted in the insets labeled as A, B, C and D, were directly and clearly resolved via the CCD captured probe pulse pattern. The diameter of the probe beam recorded on the CCD was ~10 mm, and an area of $\sim 3 \times 3$ mm² around the center of the probe beam was integrated and indicated the local intensity modulation induced by the molecular alignment. The simulated statistic metric ($\langle \langle \cos^2 \theta \rangle \rangle - 1/3$) (without Kerr and plasma contributions) of molecular O₂ (dashed curves) are also shown in Fig. 2. For the low plasma density in our experiments, the room-temperature approximation of the initial rotational population of the molecules before the excitation of the M-pulse agreed well with the measurements. The numerical simulation was done by a double averaging procedure as follows [20]. Firstly, the Schrödinger equation was solved for each initial molecular state $|\Psi$

$(t) = |J_0 M_0\rangle$, and the degree of molecular alignment at time t was acquired from the population $C_{JM}(t)$ of each rotational state as:

$$\langle \cos^2 \theta \rangle_{J_0 M_0} = \sum_{JM} C_{JM}^* C_{JM} \langle JM | \cos^2 \theta | JM \rangle. \quad (1)$$

Secondly, by assuming that initial states were populated on the basis of temperature-dependent Boltzmann distribution, we got the averaged molecular alignment degree as:

$$\langle \langle \cos^2 \theta \rangle \rangle = \frac{\sum_{J_0} P_{J_0} \sum_{M_0=-J_0}^{J_0} \langle \cos^2 \theta \rangle_{J_0 M_0}}{\sum_{J_0} P_{J_0}}, \quad (2)$$

where P_{J_0} is the population probability of the state J_0 . The simulation was done with room temperature O_2 molecules under the excitation intensity of $4.6 \times 10^{13} \text{ W/cm}^2$. This indicates that impulsive molecular alignment with distinguishable parallel/perpendicular revivals could be directly measured by spatial focusing and defocusing effects.

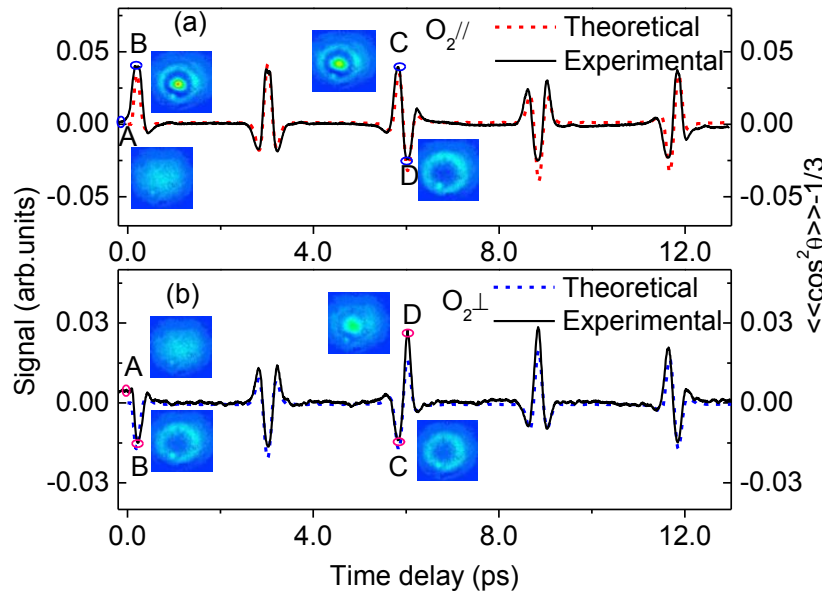


Fig. 2. Measured (solid curves) and simulated (dashed curves) molecular alignment signals of room temperature O_2 at 1 atm. when the polarization of the probe pulse is (a) parallel and (b) perpendicular to that of the M-pulse ($\sim 4.6 \times 10^{13} \text{ W/cm}^2$), represented by $O_2//$ and $O_2\perp$ respectively. The insets show the probe beam patterns captured by CCD.

Figure 3 shows the molecular alignment signals of N_2 , air, and CO_2 measured in our experiments with an excitation M-pulse intensity of $4.6 \times 10^{13} \text{ W/cm}^2$ for N_2 and air, $1.4 \times 10^{13} \text{ W/cm}^2$ for CO_2 , respectively. The measured molecular alignment degree of the parallel revival was about twice of that of the perpendicular one, which was consistent with the fact that $\langle \langle \cos^2 \theta_{//} \rangle \rangle + 2 \langle \langle \cos^2 \theta_{\perp} \rangle \rangle = 1$. The revival periods T_0 for N_2 , O_2 , and CO_2 are 8.3 ps, 11.6 ps and 42.7 ps, determined by the relation $T_0 = 1 / (2B_0c)$, respectively, where B_0 is the molecular rotational constant and c is the speed of light. As shown in Fig. 3(b), the alignment signal of air was composed of two independent revival structures of N_2 and O_2 . For different molecules, the different quarter revival structures arose from the different nuclear spin statistics of the odd and even rotational states [17].

It is well verified that the probe pulse could be focused or defocused by the spatial focusing or defocusing effects of the parallel or perpendicular molecular alignment revivals,

which increased or decreased the measured local intensity around the probe beam center. The torque induced by the M-pulse always preferentially forces molecules to align parallel to its polarization with an inertia delay of ~ 100 fs. It thus focused (defocused) the probe pulse polarized parallel (perpendicularly) to the M-pulse, leading to a positive (negative) signal around zero time delay as shown in Figs. 2 and 3. On the other hand, the M-pulse and probe pulse also experienced Kerr cross-couplings as they were temporally overlapped, leading to Kerr cross-focusing regardless of the laser polarizations. As the M-pulse and probe pulse were parallel or perpendicularly polarized, Kerr-focusing either cooperated with alignment focusing or competed with the alignment defocusing around the zero time delay. Thereafter, the molecular alignment became dominated with a time delay of one or a few hundred fs dependent upon the molecular species. Due to the inertia time delay of the alignment effects with respect to the instant Kerr effects, Kerr cross-focusing could be distinguished from alignment-induced defocusing by checking the increase or decrease of the probe pulse intensity at the center part versus the probe pulse time delay. As clearly shown in Fig. 3, for probe pulse polarized perpendicularly to the M-pulse, there were always Kerr focusing (small positive signals) before the alignment-induced defocusing (negative signals) around zero time delay. When the M-pulse and probe pulse were polarized in the parallel direction, the Kerr and alignment-induced effects established similar spatial focusing and both were summed up, making it quite difficult to distinctly separate Kerr focusing from alignment focusing, even though the Kerr coupling strength for the parallel polarized fields was about three times as that for the perpendicularly polarized fields [21].

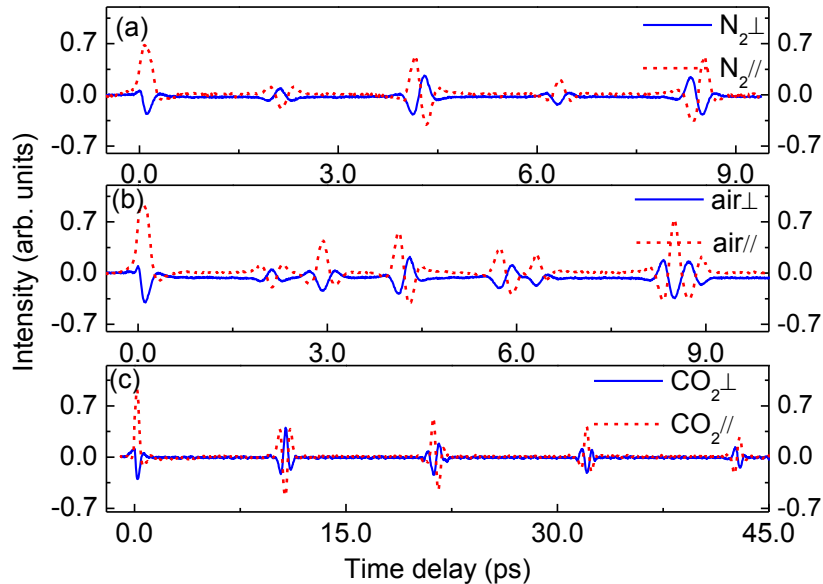


Fig. 3. Measured molecular alignment signals of (a) N_2 (b) air (c) CO_2 when the polarization of the probe pulse is perpendicular (blue-solid curves) or parallel (red-dashed curves) to that of the M-pulse ($\sim 4.6 \times 10^{13}$ W/cm 2 for N_2 and air, 1.4×10^{13} W/cm 2 for CO_2), respectively.

As shown in Figs. 2 and 3, our measurements with probe pulse polarization perpendicular to the M-pulse provided a valid way to distinguish the Kerr effect from the molecular alignment. This is more obvious for molecular CO as shown in Fig. 4(a), where the molecular alignment response was delayed about ~ 100 fs behind the Kerr effect. As shown in Fig. 4(b), the Kerr effect was not so noticeable for molecular NO by contrast with the molecular CO even both are polar molecules. This might be because that the NO (single ionization potential is ~ 9.26 eV [22]) is much easier to be ionized and only a weak M-pulse intensity of 1.3×10^{13} W/cm 2 was implemented, which was less than one third of the intensity applied to CO (single ionization potential ~ 14.01 eV [22]). Figure 4(c) illustrates the pure electronic Kerr effect in atomic gas Ar where no molecular alignment could be involved. The measured peak

amplitude ratio of the parallel/perpendicular was ~ 2.5 , which was approximate to the theoretical coefficient of 3 [21].

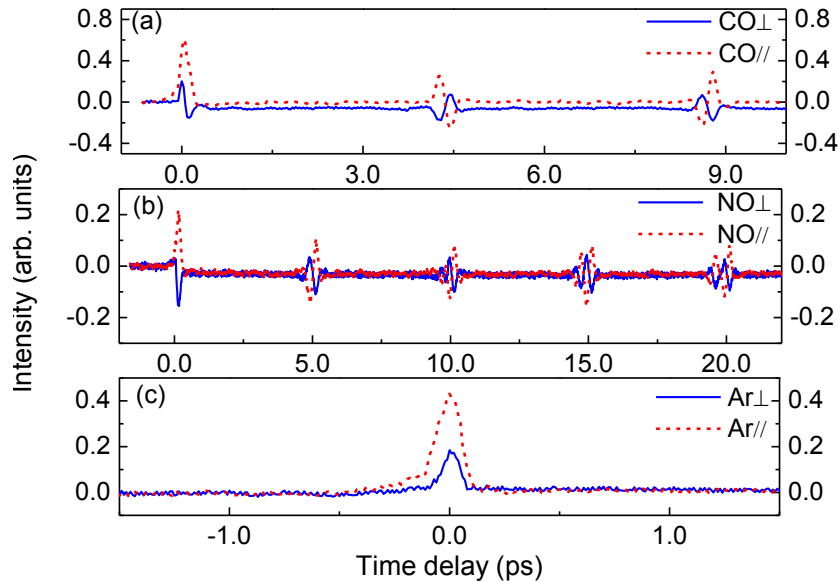


Fig. 4. Measured molecular alignment signals of (a) CO and (b) NO, and (c) Kerr effect of atomic Ar when the polarization of the probe pulse was perpendicular (blue-solid curves) and parallel (red-dashed curves) to that of the M-pulse ($\sim 4.6 \times 10^{13}$ W/cm² for CO and Ar, 1.3×10^{13} W/cm² for NO).

In addition to the Kerr and molecular alignment effects, the weak ionization induced plasma contribution was also observed. The plasma contribution always defocused the probe pulse no matter its polarization was parallel or perpendicular to that of the M-pulse. The plasma contribution was involved since it was generated by the M-pulse and slowly decayed with a typical lifetime of the order of several hundred picoseconds to a few nanoseconds depending on the plasma density. It was actually almost a constant for the short time range of several to tens ps as concerned here [14,15]. This decreased the baseline of the measured signal, as shown in the figures, which was more prominent when the M-pulse and probe pulses were polarized perpendicularly where the permanent molecular alignment impact cooperated with the plasma effect to defocus the probe pulse. Since the NO molecules are very easy to be ionized, as shown in Fig. 4(b), the plasma effect induced decrease of the molecular alignment baseline was observed even when the probe pulse polarization was parallel to the M-pulse, where the weak permanent molecular alignment effect competed with the plasma effect. Actually, the alignment degree of molecular NO was small for the weak M-pulse intensity which made the plasma effect more evident as compared with the others.

4. Conclusion

In summary, we demonstrated that the field-free molecular alignment could be directly measured by the spatial (de)focusing effects, which clearly distinguished the parallel and perpendicular revivals with increased and decreased probe pulse intensity around the beam center. Meanwhile, the Kerr and plasma effects were observed and distinguished from the molecular alignment in our measurements.

Acknowledgements

This work was partly funded by National Natural Science Fund (10990101 and 10804032), National Key Project for Basic Research (2011CB808105), Projects from Ministry of Education of China (20090076120024) and Shanghai Science and Technology Commission (09QA1402000).